

1 Zapline-plus: a Zapline extension for automatic and adaptive 2 removal of frequency-specific noise artifacts in M/EEG

3
4
5 Marius Klug^{*1} & Niels A. Kloosterman^{2,3}

6
7 ¹ Biopsychology and Neuroergonomics, Institute of Psychology and Ergonomics, Technische
8 Universität Berlin, Berlin, 10623, Germany

9 ² Max Planck UCL Centre for Computational Psychiatry and Ageing Research, Berlin,
10 Germany

11 ³ Center for Lifespan Psychology, Max Planck Institute for Human Development, Berlin,
12 Germany

13
14 * Correspondence: Marius Klug, Biopsychology and Neuroergonomics, Technische
15 Universität Berlin, Berlin, 10623, Germany
16 email: marius.klug@tu-berlin.de

17
18 Keywords: Line noise, signal processing, M/EEG, gamma oscillations, spectral analysis,
19 principal component analysis, artifact removal, preprocessing, filter

20
21 Funding: This work was supported by the DFG (GR2627/8-1) and USAF (ONR 10024807)

22
23 Running title: *Adaptive data cleaning with Zapline-plus*

24 25 **Abstract**

26
27
28
29
30
31
32
33
34
35
36
37
38
39
40
41
42
43
44
45
46
47
48
49
50
51
52
53
54
55
56
57
58
59
60
61
62
63
64
65
66
67
68
69
70
71
72
73
74
75
76
77
78
79
80
81
82
83
84
85
86
87
88
89
90
91
92
93
94
95
96
97
98
99
100
101
102
103
104
105
106
107
108
109
110
111
112
113
114
115
116
117
118
119
120
121
122
123
124
125
126
127
128
129
130
131
132
133
134
135
136
137
138
139
140
141
142
143
144
145
146
147
148
149
150
151
152
153
154
155
156
157
158
159
160
161
162
163
164
165
166
167
168
169
170
171
172
173
174
175
176
177
178
179
180
181
182
183
184
185
186
187
188
189
190
191
192
193
194
195
196
197
198
199
200
201
202
203
204
205
206
207
208
209
210
211
212
213
214
215
216
217
218
219
220
221
222
223
224
225
226
227
228
229
230
231
232
233
234
235
236
237
238
239
240
241
242
243
244
245
246
247
248
249
250
251
252
253
254
255
256
257
258
259
260
261
262
263
264
265
266
267
268
269
270
271
272
273
274
275
276
277
278
279
280
281
282
283
284
285
286
287
288
289
290
291
292
293
294
295
296
297
298
299
300
301
302
303
304
305
306
307
308
309
310
311
312
313
314
315
316
317
318
319
320
321
322
323
324
325
326
327
328
329
330
331
332
333
334
335
336
337
338
339
340
341
342
343
344
345
346
347
348
349
350
351
352
353
354
355
356
357
358
359
360
361
362
363
364
365
366
367
368
369
370
371
372
373
374
375
376
377
378
379
380
381
382
383
384
385
386
387
388
389
390
391
392
393
394
395
396
397
398
399
400
401
402
403
404
405
406
407
408
409
410
411
412
413
414
415
416
417
418
419
420
421
422
423
424
425
426
427
428
429
430
431
432
433
434
435
436
437
438
439
440
441
442
443
444
445
446
447
448
449
450
451
452
453
454
455
456
457
458
459
460
461
462
463
464
465
466
467
468
469
470
471
472
473
474
475
476
477
478
479
480
481
482
483
484
485
486
487
488
489
490
491
492
493
494
495
496
497
498
499
500
501
502
503
504
505
506
507
508
509
510
511
512
513
514
515
516
517
518
519
520
521
522
523
524
525
526
527
528
529
530
531
532
533
534
535
536
537
538
539
540
541
542
543
544
545
546
547
548
549
550
551
552
553
554
555
556
557
558
559
560
561
562
563
564
565
566
567
568
569
570
571
572
573
574
575
576
577
578
579
580
581
582
583
584
585
586
587
588
589
590
591
592
593
594
595
596
597
598
599
600
601
602
603
604
605
606
607
608
609
610
611
612
613
614
615
616
617
618
619
620
621
622
623
624
625
626
627
628
629
630
631
632
633
634
635
636
637
638
639
640
641
642
643
644
645
646
647
648
649
650
651
652
653
654
655
656
657
658
659
660
661
662
663
664
665
666
667
668
669
670
671
672
673
674
675
676
677
678
679
680
681
682
683
684
685
686
687
688
689
690
691
692
693
694
695
696
697
698
699
700
701
702
703
704
705
706
707
708
709
710
711
712
713
714
715
716
717
718
719
720
721
722
723
724
725
726
727
728
729
730
731
732
733
734
735
736
737
738
739
740
741
742
743
744
745
746
747
748
749
750
751
752
753
754
755
756
757
758
759
760
761
762
763
764
765
766
767
768
769
770
771
772
773
774
775
776
777
778
779
780
781
782
783
784
785
786
787
788
789
790
791
792
793
794
795
796
797
798
799
800
801
802
803
804
805
806
807
808
809
8010
8011
8012
8013
8014
8015
8016
8017
8018
8019
8020
8021
8022
8023
8024
8025
8026
8027
8028
8029
8030
8031
8032
8033
8034
8035
8036
8037
8038
8039
8040
8041
8042
8043
8044
8045
8046
8047
8048
8049
8050
8051
8052
8053
8054
8055
8056
8057
8058
8059
8060
8061
8062
8063
8064
8065
8066
8067
8068
8069
8070
8071
8072
8073
8074
8075
8076
8077
8078
8079
8080
8081
8082
8083
8084
8085
8086
8087
8088
8089
8090
8091
8092
8093
8094
8095
8096
8097
8098
8099
80100
80101
80102
80103
80104
80105
80106
80107
80108
80109
80110
80111
80112
80113
80114
80115
80116
80117
80118
80119
80120
80121
80122
80123
80124
80125
80126
80127
80128
80129
80130
80131
80132
80133
80134
80135
80136
80137
80138
80139
80140
80141
80142
80143
80144
80145
80146
80147
80148
80149
80150
80151
80152
80153
80154
80155
80156
80157
80158
80159
80160
80161
80162
80163
80164
80165
80166
80167
80168
80169
80170
80171
80172
80173
80174
80175
80176
80177
80178
80179
80180
80181
80182
80183
80184
80185
80186
80187
80188
80189
80190
80191
80192
80193
80194
80195
80196
80197
80198
80199
80200
80201
80202
80203
80204
80205
80206
80207
80208
80209
80210
80211
80212
80213
80214
80215
80216
80217
80218
80219
80220
80221
80222
80223
80224
80225
80226
80227
80228
80229
80230
80231
80232
80233
80234
80235
80236
80237
80238
80239
80240
80241
80242
80243
80244
80245
80246
80247
80248
80249
80250
80251
80252
80253
80254
80255
80256
80257
80258
80259
80260
80261
80262
80263
80264
80265
80266
80267
80268
80269
80270
80271
80272
80273
80274
80275
80276
80277
80278
80279
80280
80281
80282
80283
80284
80285
80286
80287
80288
80289
80290
80291
80292
80293
80294
80295
80296
80297
80298
80299
80200
80201
80202
80203
80204
80205
80206
80207
80208
80209
80210
80211
80212
80213
80214
80215
80216
80217
80218
80219
80220
80221
80222
80223
80224
80225
80226
80227
80228
80229
80230
80231
80232
80233
80234
80235
80236
80237
80238
80239
80240
80241
80242
80243
80244
80245
80246
80247
80248
80249
80250
80251
80252
80253
80254
80255
80256
80257
80258
80259
80260
80261
80262
80263
80264
80265
80266
80267
80268
80269
80270
80271
80272
80273
80274
80275
80276
80277
80278
80279
80280
80281
80282
80283
80284
80285
80286
80287
80288
80289
80290
80291
80292
80293
80294
80295
80296
80297
80298
80299
80200
80201
80202
80203
80204
80205
80206
80207
80208
80209
80210
80211
80212
80213
80214
80215
80216
80217
80218
80219
80220
80221
80222
80223
80224
80225
80226
80227
80228
80229
80230
80231
80232
80233
80234
80235
80236
80237
80238
80239
80240
80241
80242
80243
80244
80245
80246
80247
80248
80249
80250
80251
80252
80253
80254
80255
80256
80257
80258
80259
80260
80261
80262
80263
80264
80265
80266
80267
80268
80269
80270
80271
80272
80273
80274
80275
80276
80277
80278
80279
80280
80281
80282
80283
80284
80285
80286
80287
80288
80289
80290
80291
80292
80293
80294
80295
80296
80297
80298
80299
80200
80201
80202
80203
80204
80205
80206
80207
80208
80209
80210
80211
80212
80213
80214
80215
80216
80217
80218
80219
80220
80221
80222
80223
80224
80225
80226
80227
80228
80229
80230
80231
80232
80233
80234
80235
80236
80237
80238
80239
80240
80241
80242
80243
80244
80245
80246
80247
80248
80249
80250
80251
80252
80253
80254
80255
80256
80257
80258
80259
80260
80261
80262
80263
80264
80265
80266
80267
80268
80269
80270
80271
80272
80273
80274
80275
80276
80277
80278
80279
80280
80281
80282
80283
80284
80285
80286
80287
80288
80289
80290
80291
80292
80293
80294
80295
80296
80297
80298
80299
80200
80201
80202
80203
80204
80205
80206
80207
80208
80209
80210
80211
80212
80213
80214
80215
80216
80217
80218
80219
80220
80221
80222
80223
80224
80225
80226
80227
80228
80229
80230
80231
80232
80233
80234
80235
80236
80237
80238
80239
80240
80241
80242
80243
80244
80245
80246
80247
80248
80249
80250
80251
80252
80253
80254
80255
80256
80257
80258
80259
80260
80261
80262
80263
80264
80265
80266
80267
80268
80269
80270
80271
80272
80273
80274
80275
80276
80277
80278
80279
80280
80281
80282
80283
80284
80285
80286
80287
80288
80289
80290
80291
80292
80293
80294
80295
80296
80297
80298
80299
80200
80201
80202
80203
80204
80205
80206
80207
80208
80209
80210
80211
80212
80213
80214
80215
80216
80217
80218
80219
80220
80221
80222
80223
80224
80225
80226
80227
80228
80229
80230
80231
80232
80233
80234
80235
80236
80237
80238
80239
80240
80241
80242
80243
80244
80245
80246
80247
80248
80249
80250
80251
80252
80253
80254
80255
80256
80257
80258
80259
80260
80261
80262
80263
80264
80265
80266
80267
80268
80269
80270
80271
80272
80273
80274
80275
80276
80277
80278
80279
80280
80281
80282
80283
80284
80285
80286
80287
80288
80289
80290
80291
80292
80293
80294
80295
80296
80297
80298
80299
80200
80201
80202
80203
80204
80205
80206
80207
80208
80209
80210
80211
80212
80213
80214
80215
80216
80217
80218
80219
80220
80221
80222
80223
80224
80225
80226
80227
80228
80229
80230
80231
80232
80233
80234
80235
80236
80237
80238
80239
80240
80241
80242
80243
80244
80245
80246
80247
80248
80249
80250
80251
80252
80253
80254
80255
80256
80257
80258
80259
80260
80261
80262
80263
80264
80265
80266
80267
80268
80269
80270
80271
80272
80273
80274
80275
80276
80277
80278
80279
80280
80281
80282
80283
80284
80285
80286
80287
80288
80289
80290
80291
80292
80293
80294
80295
80296
80297
80298
80299
80200
80201
80202
80203
80204
80205
80206
80207
80208
80209
80210
80211
80212
80213
80214
80215
80216
80217
80218
80219
80220
80221
80222
80223
80224
80225
80226
80227
80228
80229
80230
80231
80232
80233
80234
80235
80236
80237
80238
80239
80240
80241
80242
80243
80

55 may also arise from many different sources. Recently, a novel algorithm, Zapline, was
56 introduced that combines spectral and spatial filters to isolate and remove the power line noise
57 (Cheveigné, 2019). In this paper, we present an adaptive wrapper software for Zapline to
58 enable the fully automatic removal of frequency-specific noise artifacts, including the selection
59 of noise frequencies, chunking the data into segments in which the noise is spatially stable,
60 automatically selecting the number of principal components to remove with Zapline, as well
61 as a comprehensive analysis and visualization of the cleaning and its impact on the data.
62

63 **EEG noise removal is especially difficult in mobile experiments.**

64 Mobile EEG studies require specific treatment to remove noise stemming from muscles and
65 other sources, and often independent component analysis (ICA) can be used for this (Klug
66 and Gramann, 2020). Finding the right way to remove frequency-specific noise from the data,
67 however, is a difficult task, especially since it is not necessarily spatially stable and thus can
68 have a strong negative impact on ICA. Shielding the laboratory, finding the sources and
69 eliminating them before recording the data help to alleviate the issue, but this is not always
70 feasible, and sometimes the noise goes unnoticed at first. As recent developments in EEG
71 experimental paradigms show a trend towards measuring the human in its natural habitat -
72 the world (Gramann et al., 2014) - it can become increasingly difficult or impossible to control
73 noise sources. The fields of mobile brain/body imaging (Gramann et al., 2011; Jungnickel et
74 al., 2019; Makeig et al., 2009) and neuroergonomics (Dehais et al., 2020; Raja and Matthew,
75 n.d.) use devices like virtual reality head mounted-displays, motion tracking, eye tracking,
76 treadmills, flight simulators, or actual airplanes, and more. In these experiments, participants
77 move around and interact with the world, including for example navigating through a city
78 (Wunderlich and Gramann, 2018), a virtual maze (Gehrke and Gramann, 2021), or flying an
79 airplane (Dehais et al., 2019). These data sets are almost always riddled with frequency-
80 specific noise, not only stemming from the power line but also from other devices, and often it
81 is just accepted that recordings contain noise. Removing this noise during processing is
82 especially important when comparing different conditions like seated vs. mobile experiments,
83 as different noise sources may be nearby for the different conditions, and untreated noise can
84 be wrongfully interpreted as an effect of the conditions.
85

86 **Line noise artifacts are particularly strong in MEG**

87 Magnetoencephalography (MEG) is a technique closely related to EEG, in which rather than
88 electrical activity itself, its concurrent magnetic fields are recorded (Hämäläinen et al., 1993).
89 Compared to EEG, MEG allows for better spatial specificity of (superficial) sources of neural
90 activity in the brain. Moreover, it does not require extended subject preparation and electrode
91 gel, which makes MEG more feasible for clinical populations as well as children. Magnetic
92 fields are less distorted by the skull than electrical activity, which makes MEG better suited for
93 investigating high-frequency neural activity in the so-called gamma band (although gamma is
94 investigated in EEG as well, e.g. Kloosterman et al. (2019)). However, the gamma band
95 ranges from roughly ~30 to 100 Hz (Hoogenboom et al., 2006), which encompasses the 50 or
96 60 Hz line noise (and possibly its first harmonic), to which MEG is highly sensitive and which
97 can outweigh neural activity by several orders of magnitude. This noise is often removed using
98 strong filters (see next section), which come at the cost of completely removing true neural
99 activity in this range as well. This approach hampers in-depth investigation of the function of
100 gamma activity in neural processing.
101

102 **Noise can be removed with spectral filters, regression, or spatial filters**

103 Taken together, removing frequency-specific noise is a vital part of data processing.
104 Several methods are available to remove this noise, but these all come with individual
105 drawbacks. Three main approaches can be distinguished:
106

107 (i) Spectral filters: Filtering the data with a simple low-pass or notch filter is the most
108 conventional approach. However, a low-pass filter may reduce the quality of
109 decomposing the data using Independent Component Analysis (Dimigen, 2020;

110 Hyvarinen, 1997) and a notch filter must have a steep roll-off to keep the notch
111 small, which comes with the potential of ringing artifacts (Widmann et al., 2015).
112 Additionally, both options remove all information in (or even above) the noise range
113 and will make analysis of these frequencies impossible. An approach related to
114 notch filtering is interpolation of the data in the frequency domain between directly
115 neighboring frequencies that are unaffected by the noise (e.g. 48 to 52 Hz),
116 followed by transformation of the data back into the temporal domain (Leske and
117 Dalal, 2019). This approach indeed does not introduce a deep notch in the data at
118 the line noise frequency, but nevertheless all information at the line noise frequency
119 is destroyed, rendering further analysis impossible.

120 (ii) Regression-based approaches: Regressing a target signal out of the data is
121 another often used tool. Examples are the CleanLine plugin of EEGLAB (Delorme
122 and Makeig, 2004), which uses a frequency-domain regression to remove
123 sinusoidal artifacts from the data, or TSPCA, which uses a provided reference
124 signal (Cheveigné and Simon, 2007). These approaches depend on either a
125 provided reference or a successful generation of a target signal in a given
126 frequency. Here, some noise may be left in the data, especially fluctuations in
127 amplitude or phase of the noise can be difficult to remove.

128 (iii) Spatial filters: Spatial filter options like ICA or joint diagonalization (Cheveigné and
129 Parra, 2014) are widely used and reduce noise by generating their own noise
130 reference signal from a linear combination of all channels.

131 (Cheveigné and Parra, 2014) However, noise is not always linearly separable from neural
132 activity, and thus removing noise components can inadvertently remove brain signals too.
133 These methods are also vulnerable to non-stationary of noise, which can be particularly
134 problematic in mobile EEG experiments. Finally, removing noise components from the data
135 with a spatial filter relying on linear algebra always reduces the algebraic rank of the data
136 matrix and can thus limit further analyses (Cohen, 2021). In sum, all of the above options come
137 with drawbacks.

139 **Zipline is a promising tool**

140 Recently, a promising new method that combines the spectral and spatial filtering approaches
141 to overcome some of these issues has been introduced: Zipline (Cheveigné, 2019). Zipline
142 first uses a notch filter and its complementary counterpart to split the data into the clean and
143 the noisy part, where summing them together would result in the original data. Then, the noisy
144 part is decomposed using joint decorrelation (Cheveigné and Parra, 2014) and the
145 components that carry most of the noise are removed from the noisy data. Last, the now
146 cleaned, previously noisy, data and the clean data are summed together to form the final
147 cleaned data set. This approach has the advantage of (in principle) not leaving a notch in the
148 spectrum while also not reducing the rank of the data matrix.

149 **Challenges of Zipline**

150 However, some issues remain. On the one hand, as Zipline makes use of a spatial filter, it
151 assumes a stable spatial topography of the noise over time. But especially in mobile and task-
152 based experiments the spatial distribution of the noise can change (proximity changes of
153 devices, orientation changes of the participant, touching cables, etc.). When comparing
154 different conditions, it may even be the case that some noise artifacts are entirely absent in
155 parts of the recording. This issue can lead to insufficient cleaning in some, too much cleaning
156 in other parts of the data, or the need to remove many components, which can distort the data.
157 Furthermore, a key challenge of Zipline is that it needs to be manually tuned to each data set.
158 Specifically, the following issues can be discerned:

159 (i) Finding out the correct number of components to remove. This is not
160 straightforward – recommendations range from two to four (Cheveigné, 2019), but
161 in individual cases as many as 25 components have been reported to be removed

165 (Miyakoshi et al., 2021). Presumably, the number of components depends on the
166 noise structure and number of sensors or electrodes. In our tests with high-density
167 EEG and MEG data, removing of ten to fifteen components was usually necessary
168 to contain the noise.

169 (ii) The noise frequency needs to be chosen. In most cases, choosing the power line
170 frequency is sufficient, but sometimes additional frequencies can be found, like a
171 90 Hz oscillation of a virtual reality head-mounted display, or other frequencies due
172 to additional devices in the lab. Moreover, in some of our tests Zapline proved to
173 be sensitive to even small changes in the target frequency in the range of 0.1 Hz,
174 which are hard to know in advance, especially if the frequency shifts during the
175 recording.

176
177 Taken together, Zapline is a powerful tool but requires manual parameter selection, and using
178 Zapline in an automated analysis pipeline is difficult due to this process of fine tuning.

179 180 **Zapline-plus aims to overcome Zapline's manual tuning issues**

181 We created Zapline-plus – an adaptive wrapper software for Zapline that allows fully automatic
182 use without parameter tuning. The software searches for outlier peaks in the spectrum and
183 applies Zapline to remove these. To alleviate the stationarity issue, the data is adaptively
184 segmented into chunks in which the frequency-specific noise is relatively constant, as
185 determined by the covariance structure of the data. Within each chunk, the individual chunk
186 noise peak frequency is detected, and Zapline is applied at this frequency. An adaptive
187 component detector then removes only the strongest noise components. Finally, a check of
188 the cleaning is performed and the detection process is adjusted accordingly and the procedure
189 is repeated if necessary. All used parameters and several performance indicators are stored
190 to enable an understanding and easy replication of the cleaning, and a detailed plot is created
191 to allow inspection of the cleaning performance. We tested the software on two open EEG and
192 two open MEG data sets with promising results. We discuss limitations and implications for
193 automated processing pipelines. The MATLAB source code of the software is available for
194 download at <https://github.com/MariusKlug/zapline-plus>.

195 196 **The software package**

197 In this section we describe the different aspects of the adaptive algorithm, the processing flow,
198 as well as the produced plots and the optional parameters in case the default values are
199 suboptimal.

200 201 **Algorithm**

202 Zapline-plus contains several components that are discussed in the following.
203 The processing steps include:

- 204 1. the detection of noise frequencies,
- 205 2. adaptive segmentation of the time series in chunks based on stability of the noise
206 topography,
- 207 3. applying Zapline on each segment at the detected frequency,
- 208 4. automatic detection and removal of noise components, and
- 209 5. adaptively changing and repeating the processing to prevent too weak or too strong
210 cleaning.

211
212 The processing workflow is visualized in Figure 1.

213
214 [Insert Figure 1 here]

215 216 217 **Noise frequency detection**

218 Noise frequencies are defined as frequencies having abnormally large power compared to the
219 neighboring frequencies, as determined by spectral density estimation using Welch's method
220 (Welch, 1967). We used a hanning window because it resulted in less noisy spectra than the
221 default hamming window for some data sets. The computed power spectral density (PSD)
222 values are then log transformed ($10\log_{10}$) and the mean over channels is computed
223 (corresponding to a geometric mean of the spectra that is less outlier-driven). We chose this
224 approach, because in our experience the individual channel spectra are not always normally
225 distributed, especially if there are a few very noisy outlier channels. In these cases, they mask
226 the efficacy of Zapline and hide details of the overall spectrum. Importantly, the resulting
227 geometric mean PSD is always \geq the log of the arithmetic mean PSD. Subsequently, the first
228 outlier frequency within a minimum (17 Hz) and maximum (99 Hz) frequency is searched with
229 a 6 Hz moving window. If a frequency has a difference > 4 of log PSD to the center log PSD
230 (mean of left and right thirds around the current frequency), it is found to be an outlier and the
231 search is stopped. As the input is in $10\log_{10}$ space, a difference of 4 corresponds to a 2.5-fold
232 increase of the outlier power over the center.

233

234 **Adaptive time series segmentation into chunks for cleaning**

235 Zapline detects noise components in the data using spatial principal components, and thus
236 works on the assumption of a spatial noise distribution that is stable over time. However, this
237 is not always guaranteed. Even small shifts in head orientation or a relocation of the participant
238 due to the experimental paradigm can lead to slightly different noise topography or entirely
239 new noise sources. To alleviate this issue, we implemented an adaptive method that segments
240 the data into chunks with relatively fixed noise topography. Specifically, we apply the following
241 steps:

242 1. Narrowband-filter the continuous data around the detected noise frequency ± 3
243 Hz.
244 2. Compute the channel-by-channel (i.e. sensors or electrodes) covariance matrix
245 within data epochs of one second duration.
246 3. Compute the distance between pairs of channels in successive covariance
247 matrices. This yields a measure of the change in covariance over time. A small
248 distance indicates that the noise is roughly constant, whereas a large distance
249 indicates a change in noise topography.
250 4. Determine segments (chunks) of stable noise topography by detecting peaks in the
251 covariance stationarity.

252

253 We found that this method reliably detected segments in which the noise was spatially
254 constant. However, we chose a minimum segment duration of 30 seconds to enable sufficient
255 data for the spatial decomposition employed by Zapline. Applying Zapline separately to each
256 chunk does not only allow different linear decompositions per chunk, but also allows fine-
257 tuning of the target frequency to the peak in this chunk, further improving Zapline's
258 effectiveness. Finally, this adaptive segmentation might help noise removal in cases where a
259 change in noise topography is related to an external event in task-related data that cause
260 subjects to move, such as a trial onset or the start of a short break in the experiment during
261 which the recording continues.

262

263 **Application of Zapline**

264 To detect the chunk's noise peak we first search for the peak frequency within a ± 0.05 Hz
265 range around the previously detected target frequency. We then determine a fine-grained
266 threshold to define oscillations being present or absent in that chunk: The mean of the two
267 lower 5% log PSD quantiles of the first and last third in a 6 Hz area around the target frequency
268 is computed, and the difference to the center power (mean of left and right third log PSDs
269 around the target frequency) is taken as a measure of deviation from the mean. (On a side
270 note, both the standard deviation and the median absolute deviation did not lead to good
271 results, as they can be driven by outliers to the top.) Finally, the threshold is defined as the

272 center power + 2 x deviation measure, and if the log PSD of the found peak frequency is above
273 this threshold, the chunk is found to have a noise artifact.

274
275 In the next step, cleaning is performed on a per-chunk basis using the original Zapline
276 algorithm, using either the found frequency peak and adaptive removal settings (starting with
277 3 standard deviations (SD), see section "Detection of noise components", adaptive, see
278 section "Adaptive changes"), or the original noise peak of the full data set and a fixed number
279 of components to remove (starting at 1, adaptive, see section "Adaptive changes"). We chose
280 to remove a minimum number even when no artifact was found, to make sure even missed
281 artifacts are removed while also making sure not too many components are removed in case
282 no artifact is actually present in the chunk at that frequency.

283
284 **Detection of noise components**

285 One essential parameter of Zapline is the number of to-be-removed components after sorting
286 components based on amount of explained variance. So far, this had to be chosen manually,
287 based on visual inspection of the "elbow" in the sorted components (i.e. transition from a sharp
288 to shallow drop-off). We adapted the function to include a detector for outliers in the computed
289 JD scores that represents to what extent the components load on the noise. To this end, an
290 iterative approach based on a standard mean + standard deviation (SD) threshold is used. In
291 each iteration, the detector removes outliers and then recomputes mean and SD across all
292 components, and repeats this procedure until none are left. The number of removed outliers
293 is then taken as the number of components to remove in Zapline. We found this iterative
294 approach to be more robust than an approach based on the median absolute deviation in this
295 scenario. In a final step, if the number of found outliers is less than the entered fixed removal,
296 the latter is being used, and, to prevent removing an unreasonable amount of components,
297 the number is capped at 1/5th of the components. We found a value of 3 SDs to work well in
298 most cases, but sometimes even this automatic detector removes too many or too few
299 components, which is why the SD parameter is adapted in the next step.

300
301 **Adaptive changes of the cleaning procedure**

302 After each chunk has been cleaned, the chunks are concatenated again and the cleaned
303 spectrum is computed as in section "Noise frequency detection". Although the software
304 already contains several steps to find an optimal noise reduction, the cleaning can still be too
305 weak or too strong. We implemented a check for suboptimal cleaning by using the same fine-
306 grained threshold as in section "Application of Zapline". This check is now applied to search
307 for introduced notches or remaining peaks in the power spectrum, indicating that the cleaning
308 was too strong or too weak, respectively. Specifically, if there are 0.5 % of samples of the
309 spectrum in the range of +/- 0.05 Hz around the noise frequency above the threshold of center
310 power + 2 x deviation measure, the cleaning is found to be too weak. If there are 0.5% samples
311 of the spectrum in the range of -0.4 to +0.1 Hz around the noise frequency below the threshold
312 of center power – 2 x deviation measure, the cleaning is found to be too strong. If the cleaning
313 was too weak, the SD for the number of noise components is reduced by 0.25, up to a
314 minimum of 2.5, and the fixed number of removed components (for chunks where no noise
315 was detected) is increased by 1. If the cleaning was too strong, the SD for step "Noise
316 component detection" is increased by 0.25, up to a maximum of 4, and the fixed number of
317 removed components (for chunks where no noise was detected) is decreased by 1, up to a
318 minimum of the initial fixed removal of 1. Too strong cleaning always takes precedence over
319 too weak cleaning, and if the cleaning was once found to be too strong, it can never become
320 stronger again even after it was weakened and is now found to be too weak.

321 Using these new values, the entire cleaning process of this noise frequency is re-run
322 and re-evaluated. This leads to a maximally reduced noise artifact while ensuring minimal
323 impact on any other frequencies. If no further adaptation of the cleaning needs to be
324 performed, this noise frequency is assumed to be cleaned, and the next noise frequency is
325 searched (see section "Detection of noise components") using the current noise frequency

326 +0.05 Hz as the new minimum frequency. If no other noise frequency is found, the cleaning
327 completes.

328

329 **Output figures**

330 For every frequency-specific noise artifact that is removed, a figure is generated. Example
331 plots can be seen in Figures 4 and 5. Importantly, the plot per frequency is being overwritten
332 in case the parameters are adapted, so the final plots only show the final values. These plots
333 contain all information that is necessary to determine the success of the cleaning in a
334 colorblind-friendly color scheme. The top row of the figure contains visualizations of the
335 cleaning process, the bottom row contains the final spectra and analytics information.

336

337 **[Insert Figure 2 here]**

338

339 **[Insert Figure 3 here]**

340

341 In the top row, first, the noise frequency of this iteration is shown in a zoomed-in spectrum to
342 ± 1.1 Hz around the frequency (Figure 3A). The threshold that led to the detection of this
343 frequency is shown in addition (red line), unless the detection is disabled. Next, the cleaning
344 of the individual chunks is visualized in two ways: The number of removed components per
345 chunk (Figure 3B), and the individual noise frequency detected for each chunk (Figure 3C).
346 Additionally, chunks in which no noise was detected are marked as such and the mean
347 number of removed components is denoted in the title of the plot. As each chunk contains a
348 set of components and accompanying artifact scores, this is too much to be visualized without
349 cluttering the plot, so we chose to only plot the mean artifact scores over all chunks next
350 (Figure 3D). This plot also contains the mean number of removed components (red vertical
351 line). Ideally, this line should cross the scores around the "elbow" of the curve, which indicates
352 that the outliers (i.e. the components which carry most of the noise) were detected correctly.
353 The abscissa is cut to one third of the number of components to allow the visualization of the
354 knee point. This is independent of the nkeep parameter that can be set (see section
355 "Parameters and outputs"). The SD value that was used for the detector is denoted in the title
356 of this plot. To finalize the visualization of the cleaning process, the zoomed-in spectrum of
357 the cleaned data is shown alongside the thresholds that determine if the cleaning was too
358 strong or too weak with respective horizontal lines (Figure 3E). The same y-axis is used as in
359 Figure 3A to allow comparison of pre- vs. post-cleaning. The legend of this plot also contains
360 the proportion of frequency samples that are below or above these thresholds, which
361 determines whether the cleaning needs to be adapted. It may happen that values exceeding
362 these thresholds remain, which can be either due to the minimum or maximum SD level being
363 reached or due to the fact that the cleaning would be too strong if set to a stronger level.

364 Figure 3F shows the raw spectrum as the mean of the log-transformed channel
365 spectra. Vertical shaded areas denote the minimal and maximal frequency to be checked by
366 the detector, as this can be useful to know in case a spectral peak is present in this area and
367 thus goes undetected. In Figure 3G the spectra of the cleaned (green), as well as the removed
368 data (red), are plotted. The abscissa in this plot is relative to the noise frequency which
369 facilitates distinguishing removed harmonics from other frequencies. Last, as it was shown
370 that Zapline can have undesirable effects on the spectrum below the noise frequency
371 (Miyakoshi et al., 2021), Figure 3H shows the spectra of the raw and cleaned data again
372 zoomed in to the part 10 Hz below the noise frequency to determine if this was the case. In
373 the title of Figures 3 G and H we also denote several analytics: the proportion of removed
374 power (computed on log-transformed data, corresponding to the geometric mean) of the
375 complete spectrum, of the power ± 0.05 Hz around the noise frequency, and of the power -11 Hz to -1 Hz
376 below the noise frequency, as well as the ratios of power ± 0.05 Hz around the noise frequency to the center power before and after cleaning. These plots facilitate both,
377 an understanding of the data set itself, as well as the functioning of the cleaning. Although the
378 algorithm is adaptive in many ways and should work "as is", it is naturally possible that the
379

380 noise has properties that make cleaning with Zapline-plus difficult or impossible. Hence, these
381 plots should always be inspected to determine if the cleaning was successful.
382

383 **Parameters and outputs**

384 Although we strive to provide a fully automatic solution with no need for parameter tweaking,
385 we still would like to provide options for all relevant aspects of the algorithm, including
386 switching adaptations off in case they do not work as intended. Here, we describe the
387 parameters, our reasoning for the default values and reasonable ranges, as well as the output
388 of the cleaning and additional thoughts. The data and sampling rate are required inputs, all
389 additional parameters can be entered either in key-value pairs or as a single struct:
390

- 391 - *noisefreqs* (default = empty): Vector with one or more noise frequencies to be
392 removed. If empty or missing, noise frequencies will be detected automatically.
393 Individual chunk peak detection will still be applied if set.
- 394 - *minfreq* (default = 17): Minimum frequency to be considered as noise when searching
395 for noise frequencies automatically. We chose this default as it is well above the
396 potentially problematic range of alpha oscillations (8 - 13 Hz) and also above the third
397 subharmonic of 50 Hz, which was present in some MEG data sets.
- 398 - *maxfreq* (default = 99): Maximum frequency to be considered as noise when searching
399 for noise freqs automatically. We chose this default as is is below the second
400 harmonics of the 50 Hz line noise. If the line noise cannot be removed successfully in
401 the original frequency, trying to remove the harmonics can potentially lead to
402 overcleaning.
- 403 - *adaptiveNremove* (default = true): Boolean if the automatic detection of number of
404 removed components (see section "Detection of noise components") should be used.
405 If set to false, a fixed number of components will be removed in all chunks. As this is
406 a core feature of the algorithm it is switched on by default.
- 407 - *fixedNremove* (default = 1): Fixed number of removed components per chunk. If
408 adaptiveNremove is set to true, this will be the minimum. Will be automatically adapted
409 if "adaptiveSigma" is set to true. We chose this default to remove at least one
410 component at all times, no matter whether or not a noise oscillation was detected per
411 chunk, as the detector can fail to find an oscillation that should be removed, and
412 removing a single component does not lead to a large effect if no oscillation was
413 present in the chunk.
- 414 - *detectionWinsize* (default = 6): Window size in Hz for the detection of noise peaks. As
415 the detector uses the lower and upper third of the window to determine the center
416 power (see section "Application of Zapline") this leaves a noise bandwidth of 2 Hz. In
417 our tests, some data sets indeed had such a large bandwidth of line noise, which can
418 occur if the noise varies in time.
- 419 - *coarseFreqDetectPowerDiff* (default = 4): Threshold in $10\log^{10}$ scale above the center
420 power of the spectrum to detect a peak as noise frequency. If this is too high, weaker
421 noise can go undetected and thus uncleared. If it is too low, spurious peak oscillations
422 can be wrongfully classified as noise artifacts. This default corresponds to a 2.5-fold
423 increase of the noise amplitude over the center power in the detection window which
424 worked well in our tests.
- 425 - *coarseFreqDetectLowerPowerDiff* (default = 1.76): Threshold in $10\log^{10}$ scale above
426 the center power of the spectrum to detect the end of a noise artifact peak. This is
427 necessary for the noise frequency detector to stop. This default corresponds to a 1.5
428 x increase of the noise amplitude over the center power in the detection window which
429 worked well in our tests.
- 430 - *searchIndividualNoise* (default = true): Boolean whether or not individual noise peaks
431 should be applied on the individual chunks instead of the noise frequency specified or
432 found on the complete data (see section "Application of Zapline"). As this is a core
433 feature of the algorithm it is switched on by default.

434 - *freqDetectMultFine* (default = 2): Multiplier for the 5\% quantile deviation detector of
435 the fine noise frequency detection for adaption of SD thresholds for too strong/weak
436 cleaning (see section "Application of Zapline"). If this value is lowered, the adaptive
437 changes of section "Adaptive changes of the cleaning procedure" are stricter, if it is
438 increased, these adaptations happen more rarely.
439 - *detailedFreqBoundsUpper* (default = [-0.05 0.05]): Frequency boundaries for the fine
440 threshold of too weak cleaning. This is also used for the search of individual chunk
441 noise peaks as well as the computation of analytics values of removed power and ratio
442 of noise power to surroundings. Low values mean a more direct adaptation to the peak,
443 but too low values might mean that the actual noise peaks are missed.
444 - *detailedFreqBoundsLower* (default = [-0.4 0.1]): Frequency boundaries for the fine
445 threshold of too strong cleaning. Too strong cleaning usually makes a notch into the
446 spectrum slightly below the noise frequency, which is why these boundaries are not
447 centered around the noise peak.
448 - *maxProportionAboveUpper* (default = 0.005): Proportion of frequency samples that
449 may be above the upper threshold before cleaning is adapted. We chose this value
450 since it allows a few potential outliers before adapting the cleaning.
451 - *maxProportionBelowLower* (default = 0.005): Proportion of frequency samples that
452 may be below the lower threshold before cleaning is adapted. We chose this value
453 since it allows a few potential outliers before adapting the cleaning.
454 - *noiseCompDetectSigma* (default = 3): Initial SD threshold for iterative outlier detection
455 of noise components to be removed (see section "Detection of noise components").
456 Will be automatically adapted if "adaptiveSigma" is set to 1. This value led to the fewest
457 adaptations in our tests.
458 - *adaptiveSigma* (default = 1): Boolean if automatic adaptation of
459 *noiseCompDetectSigma* should be used. Also adapts *fixedNremove* when cleaning
460 becomes stricter (see section "Adaptive changes of the cleaning procedure"). As this
461 is a core feature of the algorithm it is switched on by default.
462 - *minsigma* (default = 2.5): Minimum when adapting *noiseCompDetectSigma*. We found
463 that a lower SD than 2.5 usually resulted in removing too many components and a
464 distortion of the data.
465 - *maxsigma* (default = 4): Maximum when adapting *noiseCompDetectSigma*. We found
466 that a SD higher than 4 usually did not relax the cleaning meaningfully anymore.
467 - *chunkLength* (default = 0): Length of chunks to be cleaned in seconds. If set to 0,
468 automatic, adaptive chunking based on the data covariance matrix will be used.
469 - *minChunkLength* (default = 30): Minimum length of the chunks when adaptive
470 chunking is used. We chose a minimum chunk length of 30 s because shorter chunks
471 resulted in both, a sometimes suboptimal decomposition within Zapline and a lower
472 frequency resolution for the chunk noise peak detector. Smaller chunks result in better
473 adaptation to non-stationary noise, but also potentially worse decomposition within
474 Zapline. The necessary minimum chunk length for ideal performance may also depend
475 on the sampling rate.
476 - *winSizeCompleteSpectrum* (default = 0): Window size in samples of the *pwelch*
477 function to compute the spectrum of the complete data set for detecting the noise
478 frequencies. If 0, a window length of sampling rate x *chunkLength* is used. This
479 parameter mainly adjusts the resolution of the computed spectrum. We chose relatively
480 long windows to ensure a high resolution for the noise frequency detector.
481 - *nkeep* (default = 0): Principal Component Analysis dimension reduction of the data
482 within Zapline. If 0, no reduction will be applied. This option can be useful for extremely
483 high number of channels in which there is a risk of overfitting, but in our tests even on
484 high-density EEG and MEG data it did not lead to better results.
485 - *plotResults* (default = 1): Boolean if plot should be created.

486
487 After completing the cleaning, Zapline-plus passes out the complete configuration struct
488 including all adaptations that were applied during the cleaning. This allows a perfect replication

489 of the cleaning when applying the configuration to the same raw data again and facilitates
490 reporting the procedure. Additionally, the generated analytics values that can be found in the
491 plot are also passed out as a struct: raw and final cleaned log spectra of all channels, SD used
492 for detection, proportion of removed power of the complete spectra, the noise frequencies,
493 and below noise frequencies, ratio of noise powers to surroundings before and after cleaning
494 per noise frequency, proportion of spectrum samples above/below the threshold for each
495 frequency, matrices of number of removed components per noise frequency and chunk, of
496 artifact component scores per noise frequency and chunk, of individual noise peaks found per
497 noise frequency and chunk, and whether or not the noise peak exceeded the threshold, per
498 noise frequency and chunk. These values allow an easy check of the complete Zapline-plus
499 cleaning both for each subject and on the group-level.
500

501 **A note on the sampling rate of the data**

502 Modern M/EEG setups typically record data at high sampling rates of at least 500 Hz (1200
503 Hz is common for MEG), which allows for high temporal resolution and investigation of very
504 high frequencies. However, brain activity is typically not quantified beyond 100 Hz, and lower
505 sampling rates such as 250 Hz are typically deemed sufficient for ERP studies investigating
506 the onset of neural responses. Importantly, the presence of high frequencies in the data poses
507 a major challenge for line noise removal with Zapline, because Zapline also needs to handle
508 the (sub)-harmonics (integer divisions and multiples of the line noise frequency) that emerge
509 with frequency-specific noise. For example, at a sample rate of 1200 Hz, Zapline will remove
510 line noise at 50 Hz also at multiples of 50 Hz all the way up to 600 Hz (Nyquist frequency),
511 yielding as many as twelve harmonics. In addition, noise removal at 25 Hz (beta range) can
512 also often be observed. We noticed that Zapline performed worse with data at higher sampling
513 rates, due to the increased complexity of the data. Thus, to make Zapline's task easier, it is
514 advisable to downsample the data prior to running Zapline-plus. For the MEG data analyzed
515 here, we down-sampled to 350 Hz, for the EEG data to 250 Hz, such that only 50 and 100 Hz,
516 and 150 Hz for the MEG data, are considered for noise removal. Indeed, we found that
517 Zapline-plus performed much better at lower sampling rates.
518

519 **Example applications**

520 **Data sets**

521 In order to test the efficacy of the Zapline-plus algorithm we ran it on four different openly
522 available datasets, two EEG data sets containing both stationary and mobile conditions, and
523 two stationary MEG data sets. Notably, line noise is usually extremely strong in MEG, despite
524 extensive shielding of the equipment that is commonly applied.
525

526 **EEG study I**

527 This is an open data set available at <https://openneuro.org/datasets/ds003620/versions/1.0.2>
528 (Liebherr et al., 2021). Data of 41 participants (aged 18-39 years, M = 23.1 years, 26 female
529 and 15 male) is available, of which we only used 24 sets for technical reasons. The experiment
530 consisted of an auditory oddball task which was administered either in a laboratory
531 environment, or on a grass field, or on the campus of the University of South Australia.
532 Continuous EEG data was recorded with a 500 Hz sampling rate using 32 active Ag/AgCl
533 electrodes and the BrainVision LiveAmp (Brain Products GmbH, Gilching, Germany).
534 Electrode impedances were kept below 20k Ohm and channels were referenced to the FCz
535 electrode. See Liebherr et al. (2021) for details.
536

537 **EEG study II**

538 This is an open data set available at <http://dx.doi.org/10.14279/depositonce-10493> (Gramann
539 et al., 2021). Data of 19 participants (aged 20-46 years, mean 30.3 years, 10 female and 9
540 male) are available, which we all used. The experiment consisted of a rotation on the spot,
541 which either happened in a virtual reality environment with physical rotation or in the same
542 environment on a 2D monitor using a joystick to rotate the view. EEG data for each condition

543 was recorded with a 1000 Hz sampling rate using 157 active Ag/AgCl electrodes (129 on the
544 scalp in a custom equidistant layout, 28 around the neck in a custom neck band) and the
545 BrainAmp Move System (Brain Products GmbH, Gilching, Germany). Electrode impedances
546 were kept below 10k\$|\Omega\$ for scalp electrodes and below 50k Ohm for neck electrodes,
547 and channels were referenced to the FCz electrode. See Gramann et al. (2021) for details.
548

549 **MEG study I**

550 This open data set is available at
551 https://data.donders.ru.nl/collections/di/dccn/DSC_3011020.09_236?0 (Schoffelen et al.,
552 2019). We randomly selected 12 of the 204 subjects to test Zapline-plus. Subjects performed
553 a language task, during which they had to process linguistic utterances that either consisted
554 of normal or scrambled sentences. Four of the analyzed subjects were reading the stimuli
555 (subject IDs V1001, V1012, V1024, V1036), the other eight listened to the stimuli (subject IDs
556 A2027, A2035, A2051, A2064, A2072, A2088, A2101, A2110). Magnetoencephalographic
557 data were collected with a 275-channel axial gradiometer system (CTF). The MEG recording
558 for each subject lasted ca. 45 minutes. The signals were digitized at a sampling frequency of
559 1200 Hz (cutoff frequency of the analog anti-aliasing low pass filter was 300 Hz). See
560 Schoffelen et al. (2019) for details.
561

562 **MEG study II**

563 This data set comprises open MEG data from the Cam-CAN set of the Cambridge Centre for
564 Ageing and Neuroscience, available at <http://www.mrc-cbu.cam.ac.uk/datasets/camcan>
565 (Shafto et al., 2014; Taylor et al., 2017). We randomly selected 23 of the 647 participants.
566 Participants performed a sensory motor task on audio-visual stimuli (bilateral sine gratings
567 and concurrent audio tone). Participants were asked to respond each time a stimulus was
568 presented. The task lasted for 8 minutes and 40 seconds. Magnetoencephalographic data
569 were collected with a 306-channel Elekta Neuromag Vectorview (102 magnetometers and 204
570 planar gradiometers) at a sampling rate of 1000 Hz (bandpass 0.03-330 Hz). Only planar
571 gradiometers were used in the analysis. See Shafto et al. (2014) and Taylor et al. (2017) for
572 details.
573

574 **Processing**

575 The following preprocessing steps were applied: removal of excess channels, resampling to
576 250/350 Hz (for the EEG and MEG sets, respectively), and merging of all conditions per study
577 (EEG study II only). First, to test the different elements of the algorithm, we ran eight different
578 sets of settings on EEG study II (which contained complex artifacts that differed between the
579 two conditions):
580

- 581 1. Using a fixed removal of 3 components and no chunks, corresponding to standard
582 Zapline use.
- 583 2. Using a fixed removal, but chunking the data into 150s segments.
- 584 3. Using the automatic detector of noise components, but no chunks.
- 585 4. Combining 150s chunks and automatic noise component detector.
- 586 5. Using 150s chunks with individual peak detection and automatic noise component
587 detector.
- 588 6. Using 150s chunks without peak detection and automatic noise component
589 detection with adaptive changes for over- or undercleaning.
- 590 7. Using 150s chunks with individual peak detection, as well as automatic detection
591 with adaptive changes
- 592 8. Using all features (default): adaptive chunk length with individual peak detection,
593 as well as automatic detection with adaptive changes.

594
595 All conditions used the automatic detector of noise frequencies. With this approach we tried
596 to mimic the creation of the algorithm with successive improvements.
597

598 Subsequently, we ran Zapline-plus additionally on EEG study I and on the MEG studies. For
599 EEG study I we used only default values, for the MEG studies we set 'noisefreqs' to 50 as we
600 expected only line noise and wanted to prevent false positive noise frequency detection due
601 to very strong (sub-)harmonics of the line frequency.
602

603 **Results**

604 Overall, the cleaned spectra show that zapline-plus successfully removed the strong line noise
605 peaks while introducing only minimal notches. The results of the cleaning of all example
606 studies are depicted in Figure 4, and Table 1 lists the results for analytics for the cleaning
607 using successively enabled features for EEG study II (the number of removed components
608 per cleaning step, the ratio of noise/surroundings after cleaning, the proportion of removed
609 power below noise, and the proportion of frequency samples below and above the adaptation
610 threshold). Only EEG study II had noise frequencies different from line, which is why we
611 specifically show the raw and clean 50 Hz / surroundings power ratios. Table 2 shows the
612 results for the four example datasets (the final SD value for detection, the number of removed
613 components per cleaning step, the ratio of noise/surroundings before and after cleaning, and
614 the proportion of removed power below noise).
615

616 [Insert Table 1 here]
617

618 [Insert Table 2 here]
619

620 **Suboptimal case results**

621 Viewing only the average results of the final cleaning, however, yields only a limited
622 understanding of the detailed processes. Some data sets had less-than-ideal results, for
623 example they showed a distortion of the spectrum below noise such that the power was
624 actually increased. This could be seen mostly in data sets with particularly strong noise
625 contamination, especially in MEG study I where four data sets had more than 800 times
626 stronger power at noise frequency than surroundings, up to almost 7000 times for the noisiest
627 data set (Figure 4, MEG study I, right panel). All these four data sets, but only them, exhibited
628 a negative removal of power below noise, i.e. an increase of power in the cleaned data, and
629 they drive the average that can be seen in Table 2 and Figure 4, MEG study I, left panel (green
630 line above black). Also, while all data sets showed a reduction in power of the noise, some of
631 them had comparably strong residual noise peaks (ratios of noise/surroundings above 1.2,
632 these usually also had very high ratios before cleaning), indicating that Zapline-plus could not
633 fully clean these data sets.
634

635 [Insert Figure 4 here]
636

637 **Zapline-plus does not affect phase angle of the signal**

638 Zapline-plus removes frequency-specific artifacts using the data's power spectrum, but it is
639 unknown to what extent the phase angle of the remaining signal at the cleaned frequency is
640 affected by the cleaning process. Assuming that frequency-specific noise such as line noise
641 is strongly oscillatory and thus has a steady circular progression of phase angle over time, we
642 asked whether Zapline-plus indeed strictly removes a noise time course with such a steady
643 phase from the contaminated signal.
644

645 To address this question, we computed the 50 Hz oscillatory phase and power of the
646 noise time series, as generated by Zapline-plus for removal from a chunk of 50-Hz
647 contaminated MEG data (duration 543 s). We then used the peaks in the sawtooth-like 50 Hz
648 phase time series (i.e. where phase was at 2π) to segment the time-domain noise data into
649 "trials" of 2001 samples (5.7 s duration), and averaged the trials. Due to time-locking to the
650 2π phase angle of the 50 Hz oscillation, this resulted in a strong, oscillatory average time
651 course (Figure 5A), which we confirmed to be at exactly 50 Hz (Figure 5B). We reasoned that
any phase irregularities in the trial-average time series would result in an average power drop-

652 off towards the trial borders due to reduced time-locking further away from time zero. Visual
653 inspection of Figure 5B does not reveal such a drop-off (see Figure 5A, oscillation equally
654 strong at all time points), suggesting that the phase angle of the 50 Hz artifact was constant
655 throughout the noise time series. Note that we cut the time axis of the figure because the
656 edges did not contain time-frequency data.

657 To quantify the stability of the 50 Hz phase angle, we then computed the inter-trial
658 phase coherence (ITPC) for each time point. ITPC is an established measure of phase stability
659 that ranges between 0 (highly variable phase angle across trials at a given time point) and 1
660 (exact same phase) (Tallon-Baudry et al., 1996). We expected 50 Hz ITPC to reach its peak
661 at time zero, because the trials were aligned to a fixed phase angle (2π) at this timepoint –
662 and fall off at towards the trial boundaries due to any phase irregularities occurring from trial
663 to trial. This inverted-U shape is indeed what we found (purple line in Figure 5C). Crucially,
664 however, 50-Hz ITPC dropped only ca. 1% at the trial borders, (0.4 s from time zero,
665 corresponding to 20 periods), ITPC=0.965 vs. 0.954, indicating that the phase of the 50 Hz
666 oscillation in the noise data was very stable over time. ITPC of frequencies around 50 Hz was
667 consistently low (ITPC < 0.06, cyan lines in Figure 5, right), as expected since the trials were
668 strictly based on the 50 Hz phase angle. This suggests that Zapline-plus removes a very
669 rhythmically stable 50 Hz oscillation from the raw signal. We conclude that the phase of 50 Hz
670 activity remaining in the data after line noise removal with Zapline-plus (e.g. gamma activity)
671 can be assumed to be unaffected, and can thus safely be used in subsequent analysis.

672
673 [Insert Figure 5 here]
674

675 Discussion

676 In this work, we extended Zapline to allow fully automatic removal of line noise and other
677 spectral peaks, while giving the user a maximum of flexibility and information, as well as
678 allowing complete replicability of the processing. We evaluated the algorithm on two EEG and
679 two MEG data sets. First, we checked whether the different parts of the algorithm improved
680 the cleaning on one EEG study, then we applied the final default values to the three other
681 datasets. Taken together, the results show that the new features allow for fully automatic noise
682 removal and make the algorithm applicable for different kinds of electrophysiological data,
683 resulting in a substantial decrease of frequency-specific noise with minimal negative impact
684 on true neural activity.

685 Efficacy of the algorithm

686 Examination of the algorithm components on EEG study II showed that they do improve the
687 results. However, the improvement is not a simple linear relationship. Both, using fixed 150s
688 chunks, and using automatic detection of to-be-removed components improved the clean ratio
689 of noise/surrounding power similarly over using the standard fixed approach. In doing so, using
690 auto detection affected the power below noise frequencies (-11 to -1 Hz) more than chunks
691 did, but chunks had a larger proportion of samples below the threshold directly at the noise
692 frequency, meaning chunks introduced a slight notch into the spectrum, whereas auto cleaning
693 without chunks distorted the spectrum more generally. Interestingly, combining these two
694 approaches led to the lowest ratio of noise/surroundings power while also introducing
695 substantial amounts of overcleaning, both in terms of general distortion (% removed below
696 noise) and a notch (% below lower threshold). This combination also had the fewest samples
697 above the adaptation threshold, corresponding to the low noise/surroundings ratio.

698 The strong overcleaning effect can be explained by the fact that not all noise
699 oscillations were present in all chunks. Although the automatic detection of components to
700 remove should be able to select fewer samples with less noise, it requires some sort of 'knee-
701 point' or 'corner' in the artifact scores. In chunks with no oscillation in the given noise
702 frequency, the scores exhibit an almost linear decrease, which can lead to erroneously
703 removing large numbers of components. This negative interaction effect can be fixed by either
704 adapting the SD level the detector uses, or by simply not using auto detection when no noise

706 is present. Using either improvement alone led to similar levels of cleaning in terms of
707 noise/surroundings power as well as % of samples above threshold, while the adaptive
708 cleaning had a slightly reduced impact on the spectrum below noise and a reduced notch.
709 Combining all options, chunks with individual peak detection, as well as automatic detection
710 with adaptation, led to even better overall results.

711 Last, adding the adaptive variable chunk length based on the spatial stability of the
712 noise (using the full feature set of the algorithm) improved the specificity of the cleaning even
713 further. This combination had a lower % of samples below and above the adaptation threshold
714 and a lower impact to the spectrum below noise. Overall, the combination of all features of the
715 algorithm successfully cleans the data, while keeping the distortions to the spectrum as low
716 as possible.

717 Applying this final combination to all example data sets led to substantial improvements
718 of the spectra. In EEG study I, there was 50 Hz line noise present in the data, and an unknown
719 oscillation at around 7 Hz, plus harmonics. The former was detected and successfully cleaned
720 by Zapline-plus, whereas the latter was too small to be detected. EEG study II is a particularly
721 heavily contaminated study, as can be seen by the various peaks in the spectrum. However,
722 Zapline-plus was able to successfully clean these data, not only at line noise, but also all other
723 strong peaks. This example emphasizes the importance of the automatic noise frequency
724 detector, as these oscillations are difficult to anticipate.

725 Applying Zapline-plus on the MEG studies shows that even extremely noisy data is
726 successfully cleaned. It can be seen in MEG study I, however, that Zapline-plus may have an
727 impact on the overall spectrum by increasing the broadband power. This effect is driven by
728 four of the twelve data sets, which show extreme levels of noise before cleaning, the other
729 eight do not show such an increase. In these cases the actual impact of the cleaning on final
730 measures must be closely examined in order to decide whether the trade-off of reduced noise
731 vs. spectrum distortions is worth it in this particular analysis or if the cleaning must be adapted.
732

733 **Other notes**

734 In EEG study II, it was clearly visible that some noise frequencies were only present in the first
735 or second part of the data (body vs joystick rotation, see Figure 3 for an example of a noise
736 frequency only present in the second half). This underlines the importance of the chunking
737 and individual frequency detection, as this allows checking whether the oscillation is actually
738 present in that chunk and prevent overcleaning. We would also like to point out the importance
739 of fine-tuned noise frequency detection for some frequencies, especially the one seen in
740 Figure 3. The separation of 20.9 Hz and, subsequently, 21.1 Hz noise is important as the two
741 frequencies can not be cleaned together. This would be impossible to see without a high
742 resolution of the frequency spectrum, and simply cleaning with a fixed 21 Hz setting does lead
743 to subpar results. Also, as can be seen in Figure 2 the peak frequency of the line noise is not
744 always stationary and Zapline-plus is able to detect these variations.

745

746 **Limitations**

747 As we showed, the cleaning is not always perfect. Especially with data that is heavily
748 contaminated with noise, it is possible to 1) change the spectrum below the noise frequency
749 such that the power is actually increased, 2) leave residual noise in the data, or 3) after
750 cleaning, leave a small notch in the spectrum. Although the default values of the algorithm are
751 chosen to fit most of the data sets, in some cases it might be better to adjust them according
752 to the results obtained from the automatic cleaning and then re-run Zapline-plus. The user is
753 strongly advised to always check the resulting analytics plots after applying Zapline-plus.

754

755 **Future directions**

756 It might also be that no matter the parameter adjustment, the cleaning will remain suboptimal.
757 In these cases it could be useful to combine Zapline-plus with CleanLine, since these two
758 methods rely on distinct, complementary algorithms to isolate and remove line noise. Zapline,
759 on the one hand, applies a fixed spatial filter over the entire data segment, allowing it to

760 account for variations in noise amplitude in the temporal domain, but strictly not changes in
761 noise topography. Cleanline, in contrast, removes a fixed oscillatory noise signal in the time-
762 domain data in each channel separately, allowing full flexibility in the spatial, but not the
763 temporal domain. Indeed, a recent paper shows that combining the two methods can improve
764 the cleaning of heavily contaminated data (Miyakoshi et al., 2021). Examining the possibility
765 of an automatic extra CleanLine step if Zapline-plus alone yielded suboptimal results would
766 be an option for future investigations.

767 Another interesting possibility is to visualize the topographies of the removed artifacts.
768 As Zapline internally uses spatial filters, these can be visualized like any other spatial filter and
769 be added to the analytics information feedback for the user. However, this is not
770 straightforward as Zapline-plus specifically uses different spatial decompositions and different
771 number of removed components for each chunk. Still, if the filters vary only slightly, visualizing
772 the average of the removed topographies could be valuable feedback.

773 Lastly, it could be explored whether Zapline-plus can also be used for other
774 applications. For example, some of our tests suggest that one could remove very regular
775 mechanical walking artifacts in mobile EEG studies, or the steps could be extracted to create
776 events for subsequent analysis. Another option would be to extract alpha oscillations (8-13
777 Hz) that exceed the 1/f background activity. This topic has already been mentioned in the
778 original Zapline paper (Cheveigné, 2019), but with a focus on removing alpha for other
779 analysis. Extracting only the oscillatory alpha time series by switching the "clean" with the
780 "noise" data could result in more specific alpha signals than using a standard band-pass filter.
781 In sum, Zapline-plus is essentially a tool created for noise removal, but it can also be used to
782 extract all kinds of oscillatory activity to be used in other analyses, which makes it a versatile
783 tool in any analysis pipeline.

784 785 **Implications for the field**

786 Removing line noise is an undeniably important part of electrophysiological data processing,
787 and having the option to do so without risking the analysis of potentially important frequencies
788 while retaining full data rank is a valuable tool. The newly added features of fully automatic
789 and documented processing including the detection of noise oscillations are especially
790 important considering the current trend towards complete automatic processing pipelines
791 (Bigdely-Shamlo et al., 2015; Cruz et al., 2018; Gabard-Durnam et al., 2018; Pedroni et al.,
792 2019) and the need for more rigorous methods in neurophysiological analysis (Cohen, 2017)
793 due to the replication crisis (Collaboration, 2015). Also, although the impact of preprocessing
794 has been investigated in parts (Robbins et al., 2020), and some pipelines create
795 comprehensive documentation of their processes, a documentation of the line noise removal
796 as detailed as provided by Zapline-plus is lacking thus far. Zapline-plus contributes to the field
797 by making the removal of line noise and other oscillation artifacts in large data sets automatic,
798 easy, transparent, and reproducible, while limiting its potential negative impact on downstream
799 analysis. It can easily be integrated in any automatic processing pipeline.

800 801 **Acknowledgements**

802 We are thankful to the researchers who made the data sets freely available and to Alain de
803 Cheveigné who kindly allowed the adaptation and re-hosting of parts of the original Zapline
804 code. We would also like to thank the members of the Berlin Mobile Brain/Body Imaging Lab
805 of Prof. Klaus Gramann for valuable discussions throughout the development of the algorithm.
806 We acknowledge the support of this work by the DFG (GR2627/8-1) and USAF (ONR
807 10024807).

808 809 **Conflict of interest**

810 The authors declare no conflict of interest.

811 812 **Data availability statement**

813 The data used in this study is available for download as laid out in the Datasets section. The
814 MATLAB source code of the software is available for download at
815 <https://github.com/MariusKlug/zapline-plus>.

816

817 **References**

818

819

820 Bigdely-Shamlo N, Mullen T, Kothe C, Su K-M, Robbins KA. 2015. The PREP pipeline:
821 standardized preprocessing for large-scale EEG analysis. *Front Neuroinform* 9:16.
822 doi:10.3389/fninf.2015.00016

823 Cheveigné A de. 2019. ZapLine: A simple and effective method to remove power line
824 artifacts. *Neuroimage* 116356. doi:10.1016/j.neuroimage.2019.116356

825 Cheveigné A de, Parra LC. 2014. Joint decorrelation, a versatile tool for multichannel data
826 analysis. *Neuroimage* 98:487–505. doi:10.1016/j.neuroimage.2014.05.068

827 Cheveigné A de, Simon JZ. 2007. Denoising based on time-shift PCA. *J Neurosci Meth*
828 165:297–305. doi:10.1016/j.jneumeth.2007.06.003

829 Cohen M. 2021. Linear Algebra: Theory, Intuition, Code.

830 Cohen MX. 2017. Rigor and replication in time-frequency analyses of cognitive
831 electrophysiology data. *Int J Psychophysiol* 111:80–87.
832 doi:10.1016/j.ijpsycho.2016.02.001

833 Collaboration OS. 2015. PSYCHOLOGY. Estimating the reproducibility of psychological
834 science. *Sci New York N Y* 349:aac4716. doi:10.1126/science.aac4716

835 Cruz JR da, Chicherov V, Herzog MH, Figueiredo P. 2018. An automatic pre-processing
836 pipeline for EEG analysis (APP) based on robust statistics. *Clin Neurophysiol* 129:1427–
837 1437. doi:10.1016/j.clinph.2018.04.600

838 Dehais F, Duprè A, Blum S, Drougard N, Scannella S, Roy RN, Lotte F. 2019. Monitoring
839 Pilot's Mental Workload Using ERPs and Spectral Power with a Six-Dry-Electrode EEG
840 System in Real Flight Conditions. *Sensors* 19:1324. doi:10.3390/s19061324

841 Dehais F, Lafont A, Roy R, Fairclough S. 2020. A Neuroergonomics Approach to Mental
842 Workload, Engagement and Human Performance. *Front Neurosci-switz* 14:268.
843 doi:10.3389/fnins.2020.00268

844 Delorme A, Makeig S. 2004. EEGLAB: an open source toolbox for analysis of single-trial
845 EEG dynamics including independent component analysis. *J Neurosci Meth* 134:9–21.
846 doi:10.1016/j.jneumeth.2003.10.009

847 Dimigen O. 2020. Optimizing the ICA-based removal of ocular EEG artifacts from free
848 viewing experiments. *Neuroimage* 207:116117. doi:10.1016/j.neuroimage.2019.116117

849 Gabard-Durnam LJ, Leal ASM, Wilkinson CL, Levin AR. 2018. The Harvard Automated
850 Processing Pipeline for Electroencephalography (HAPPE): Standardized Processing
851 Software for Developmental and High-Artifact Data. *Front Neurosci-switz* 12:97.
852 doi:10.3389/fnins.2018.00097

853 Gehrke L, Gramann K. 2021. Single-trial regression of spatial exploration behavior indicates
854 posterior EEG alpha modulation to reflect egocentric coding. *Eur J Neurosci* 54:8318–
855 8335. doi:10.1111/ejn.15152

856 Gramann K, Ferris DP, Gwin J, Makeig S. 2014. Imaging natural cognition in action. *Int J*
857 *Psychophysiol* 91:22–29. doi:10.1016/j.ijpsycho.2013.09.003

858 Gramann K, Gwin JT, Ferris DP, Oie K, Jung T-P, Lin C-T, Liao L-D, Makeig S. 2011.
859 Cognition in action: imaging brain/body dynamics in mobile humans. *Rev Neuroscience*
860 22:593–608. doi:10.1515/rns.2011.047

861 Gramann K, Hohlefeld FU, Gehrke L, Klug M. 2021. Human cortical dynamics during full-
862 body heading changes. *Sci Rep-uk* 11:18186. doi:10.1038/s41598-021-97749-8

863 Hämäläinen M, Hari R, Ilmoniemi RJ, Knuutila J, Lounasmaa OV. 1993.
864 Magnetoencephalography—theory, instrumentation, and applications to noninvasive
865 studies of the working human brain. *Rev Mod Phys* 65:413–497.
866 doi:10.1103/revmodphys.65.413

867 Hoogenboom N, Schoffelen J-M, Oostenveld R, Parkes LM, Fries P. 2006. Localizing human
868 visual gamma-band activity in frequency, time and space. *Neuroimage* 29:764 773.
869 doi:10.1016/j.neuroimage.2005.08.043

870 Hyvärinen A. 1997. A family of fixed-point algorithms for independent component analysis.
871 1997 *ieee Int Conf Acoust Speech Signal Process* 5:3917–3920 vol.5.
872 doi:10.1109/icassp.1997.604766

873 Jungnickel E, Gehrke L, Klug M, Gramann K. 2019. Neuroergonomics 59–63.
874 doi:10.1016/b978-0-12-811926-6.00010-5

875 Kloosterman NA, Gee JW de, Werkle-Bergner M, Lindenberger U, Garrett DD, Fahrenfort
876 JJ. 2019. Humans strategically shift decision bias by flexibly adjusting sensory evidence
877 accumulation. *Elife* 8:e37321. doi:10.7554/elife.37321

878 Klug M, Gramann K. 2020. Identifying key factors for improving ICA-based decomposition of
879 EEG data in mobile and stationary experiments. *Eur J Neurosci*. doi:10.1111/ejn.14992

880 Leske S, Dalal SS. 2019. Reducing power line noise in EEG and MEG data via spectrum
881 interpolation. *Neuroimage* 189:763–776. doi:10.1016/j.neuroimage.2019.01.026

882 Liebherr M, Corcoran AW, Alday PM, Coussens S, Bellan V, Howlett CA, Immink MA, Kohler
883 M, Schlesewsky M, Bornkessel-Schlesewsky I. 2021. EEG and behavioral correlates of
884 attentional processing while walking and navigating naturalistic environments. *Sci Rep-uk*
885 11:22325. doi:10.1038/s41598-021-01772-8

886 Makeig S, Gramann K, Jung T-P, Sejnowski TJ, Poizner H. 2009. Linking brain, mind and
887 behavior. *Int J Psychophysiol* 73:95–100. doi:10.1016/j.ijpsycho.2008.11.008

888 Miyakoshi M, Schmitt LM, Erickson CA, Sweeney JA, Pedapati EV. 2021. Can We Push the
889 “Quasi-Perfect Artifact Rejection” Even Closer to Perfection? *Front Neuroinform*
890 14:597079. doi:10.3389/fninf.2020.597079

891 Pedroni A, Bahreini A, Langer N. 2019. Automagic: Standardized preprocessing of big EEG
892 data. *Neuroimage* 200:460–473. doi:10.1016/j.neuroimage.2019.06.046

893 Raja P, Matthew R. n.d. Neuroergonomics: The brain at work. Oxford University Press.

894 Robbins KA, Touryan J, Mullen T, Kothe C, Bigdely-Shamlo N. 2020. How Sensitive Are
895 EEG Results to Preprocessing Methods: A Benchmarking Study. *Ieee T Neur Sys Reh*
896 28:1081–1090. doi:10.1109/tnsre.2020.2980223

897 Schoffelen J-M, Oostenveld R, Lam NHL, Uddén J, Hultén A, Hagoort P. 2019. A 204-
898 subject multimodal neuroimaging dataset to study language processing. *Sci Data* 6:17.
899 doi:10.1038/s41597-019-0020-y

900 Shafto MA, Tyler LK, Dixon M, Taylor JR, Rowe JB, Cusack R, Calder AJ, Marslen-Wilson
901 WD, Duncan J, Dagleish T, Henson RN, Brayne C, Matthews FE, Cam-CAN. 2014. The
902 Cambridge Centre for Ageing and Neuroscience (Cam-CAN) study protocol: a cross-
903 sectional, lifespan, multidisciplinary examination of healthy cognitive ageing. *Bmc Neurol*
904 14:204. doi:10.1186/s12883-014-0204-1

905 Taylor JR, Williams N, Cusack R, Auer T, Shafto MA, Dixon M, Tyler LK, Cam-CAN, Henson
906 RN. 2017. The Cambridge Centre for Ageing and Neuroscience (Cam-CAN) data
907 repository: Structural and functional MRI, MEG, and cognitive data from a cross-sectional
908 adult lifespan sample. *Neuroimage* 144:262–269. doi:10.1016/j.neuroimage.2015.09.018

909 Welch P. 1967. The use of fast Fourier transform for the estimation of power spectra: A
910 method based on time averaging over short, modified periodograms. *Ieee T Acoust
911 Speech* 15:70–73. doi:10.1109/tau.1967.1161901

912 Widmann A, Schröger E, Maess B. 2015. Digital filter design for electrophysiological data – a
913 practical approach. *J Neurosci Meth* 250:34 46. doi:10.1016/j.jneumeth.2014.08.002

914 Wunderlich A, Gramann K. 2018. Electrocortical Evidence for Long-Term Incidental Spatial
915 Learning Through Modified Navigation Instructions. *Biorxiv* 280842. doi:10.1101/280842

916
917 **Tables**
918

	1. original Zapline	2. fixed chunks	3. auto comp. detection	4. auto + fixed chunks
final # of removed components	3 (0)	3 (0)	4.55 (1.93)	5.76 (1.61)
clean ratio nois/surroundings	1.22 (0.21)	1.09 (0.12)	1.08 (0.04)	0.97 (0.07)
% removed power below noise	1.73 (0.57)	1.87 (0.46)	3.05 (2.10)	4.30 (1.36)
% below lower threhsold	0 (0)	3.36 (6.67)	0.20 (0.63)	20.08 (16.78)
% above upper threshold	23.13 (11.37)	16.79 (13.67)	14.74 (9.94)	6.82 (7.06)
	5. auto + fixed chunks + peaks	6. auto + adaptive + fixed chunks	7. auto + adaptive + fixed chunks + peaks	8 .auto + adaptive + variable chunks + peaks

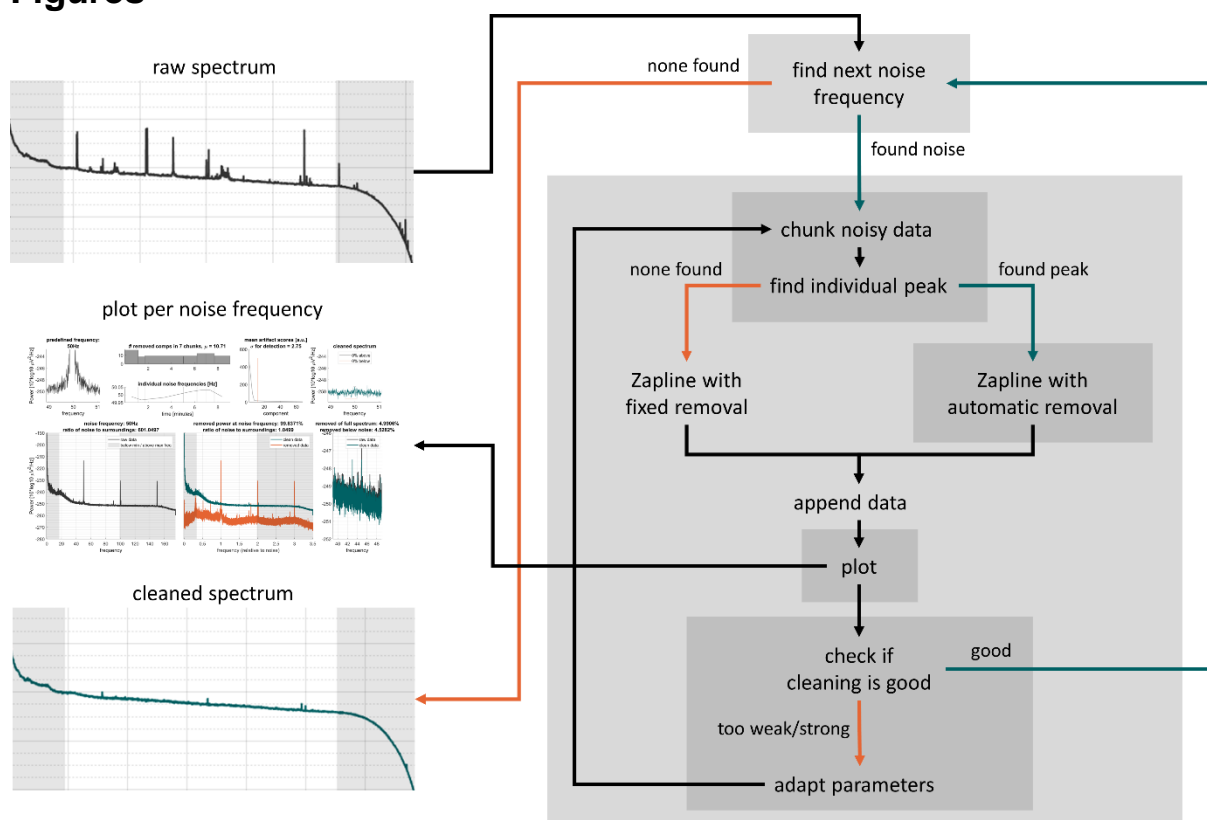
final # of removed components	4.08 (1.09)	3.63 (0.88)	3.31 (0.92)	3.20 (0.78)
clean ratio noise/surroundings	1.00 (0.05)	1.01 (0.05)	1.03 (0.04)	1.03 (0.08)
% removed power below noise	3.01 (0.95)	2.41 (0.72)	2.20 (0.69)	2.12 (1.92)
% below lower threhsold	9.31 (12.84)	5.26 (11.01)	2.94 (6.51)	0.36 (1.44)
% above upper threshold	7.25 (7.90)	8.33 (6.85)	8.37 (7.47)	5.64 (10.81)

919 **Table 1 | Algorithm steps applied to an example dataset.** Analytics (mean and standard
 920 deviation) when using varying features enabled during cleaning of EEG study II. The removed
 921 power below noise refers to -11 Hz to -1 Hz below the detected noise frequency, the
 922 percentage below/above thresholds refer to the proportion of samples in the spectrum
 923 exceeding the thresholds for fine-grained adaptation. Although they were not always used,
 924 they are always available for analysis. The values are first averaged over all detected noise
 925 frequencies per subject. “1. original Zapline” refers to the basic fixed version of Zapline, “2.
 926 fixed chunks” refers to applying the basic Zapline on regular 150s chunks, “3. auto comp.
 927 detection” refers to using automatic detection of components to remove, “4. auto + fixed
 928 chunks” refers to using automatic noise component detection on regular 150s chunks, “5. auto
 929 + fixed chunks + peaks” refers to using automatic noise component detection on regular 150s
 930 chunks with individual chunk noise peak detection, “6. auto + adaptive + fixed chunks” refers
 931 to using automatic noise detection on regular 150s chunks with adaptive detection strength,
 932 “7. auto + adaptive + fixed chunks + peaks” refers to using automatic noise component
 933 detection on regular 150s chunks with individual peak detection and adaptive detection
 934 strength, and “8. auto + adaptive + variable chunks + peaks” refers to using automatic noise
 935 component detection on automatically detected variable chunks with individual peak detection
 936 and adaptive detection strength (see also section “Processing”). N = 19.
 937

	EEG study I (N = 24)	EEG study II (N = 19)	MEG study I (N = 12)	MEG study II (N = 23)
final SD of detector	2.63 (0.18)	3.10 (0.40)	3.42 (0.73)	3.38 (0.61)
final # of removed components	2.83 (0.95)	3.20 (0.78)	17.18 (8.62)	8.21 (3.66)
raw ratio noise/surroundings	6.99 (6.26)	2.40 (1.91)	962.6 (1799.6)	232.6 (369.4)
clean ratio noise/surroundings	1.22 (0.17)	1.03 (0.08)	1.32 (0.61)	1.00 (0.05)
% of removed power below noise	6.20 (2.60)	2.12 (1.92)	-31.34 (75.71)	3.52 (1.38)

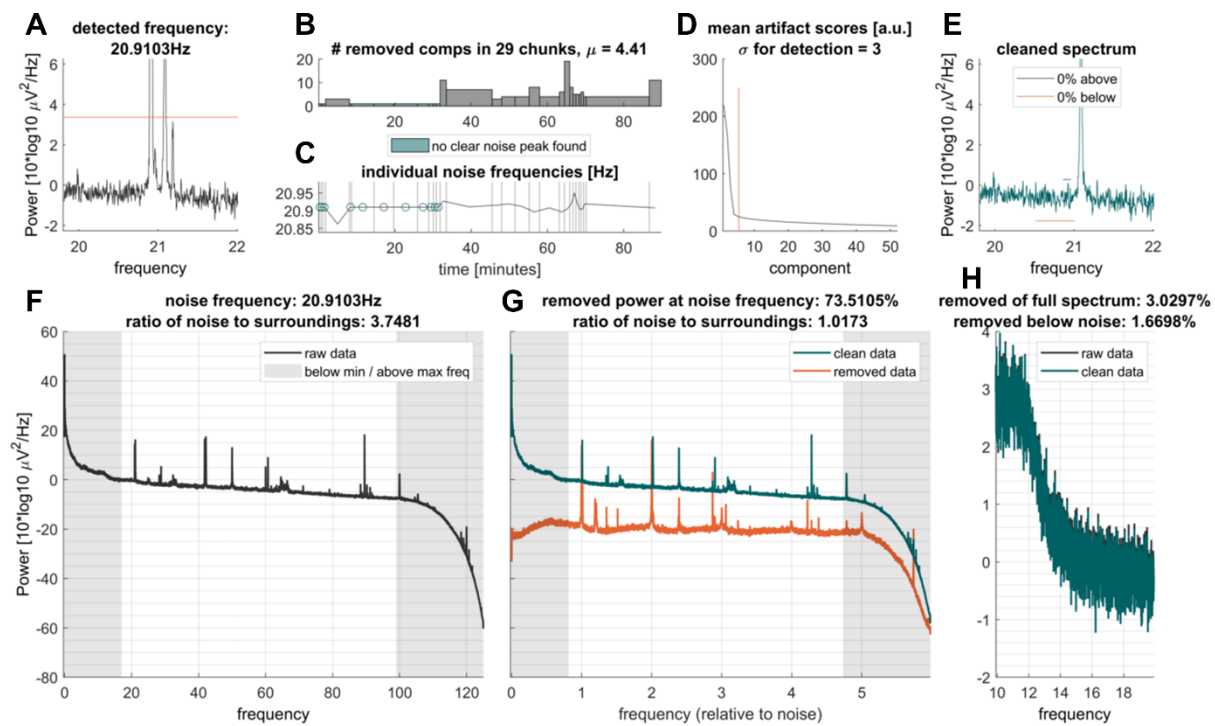
938 **Table 2 |** Analytics results of the cleaning of four openly available data sets (mean and
 939 standard deviation). The removed power below noise refers to -11 Hz to -1 Hz below the
 940 detected noise frequency. For EEG study II the values are first averaged over all detected
 941 noise frequencies per subject, the other studies had only 50 Hz line noise removed.
 942

943 **Figures**



944
945
946
947
948
949

Figure 1 | Processing flow of the Zapline-plus algorithm. Please see the text for details about the individual steps.

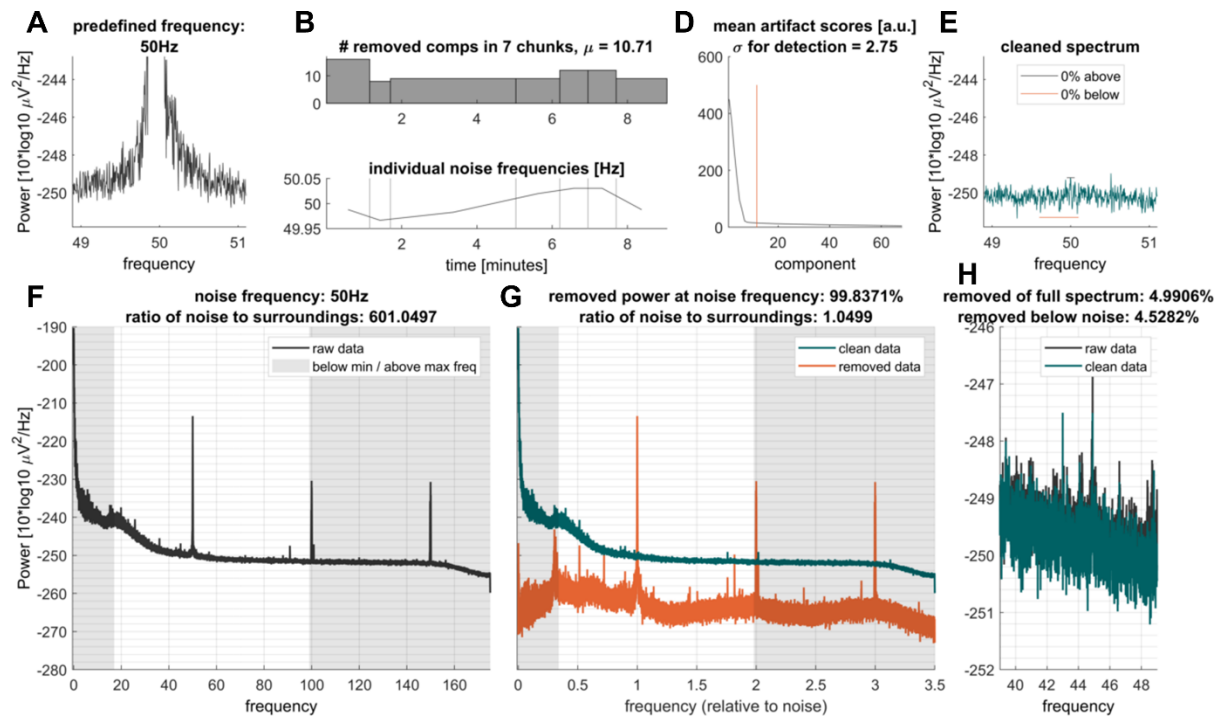


950
951
952
953

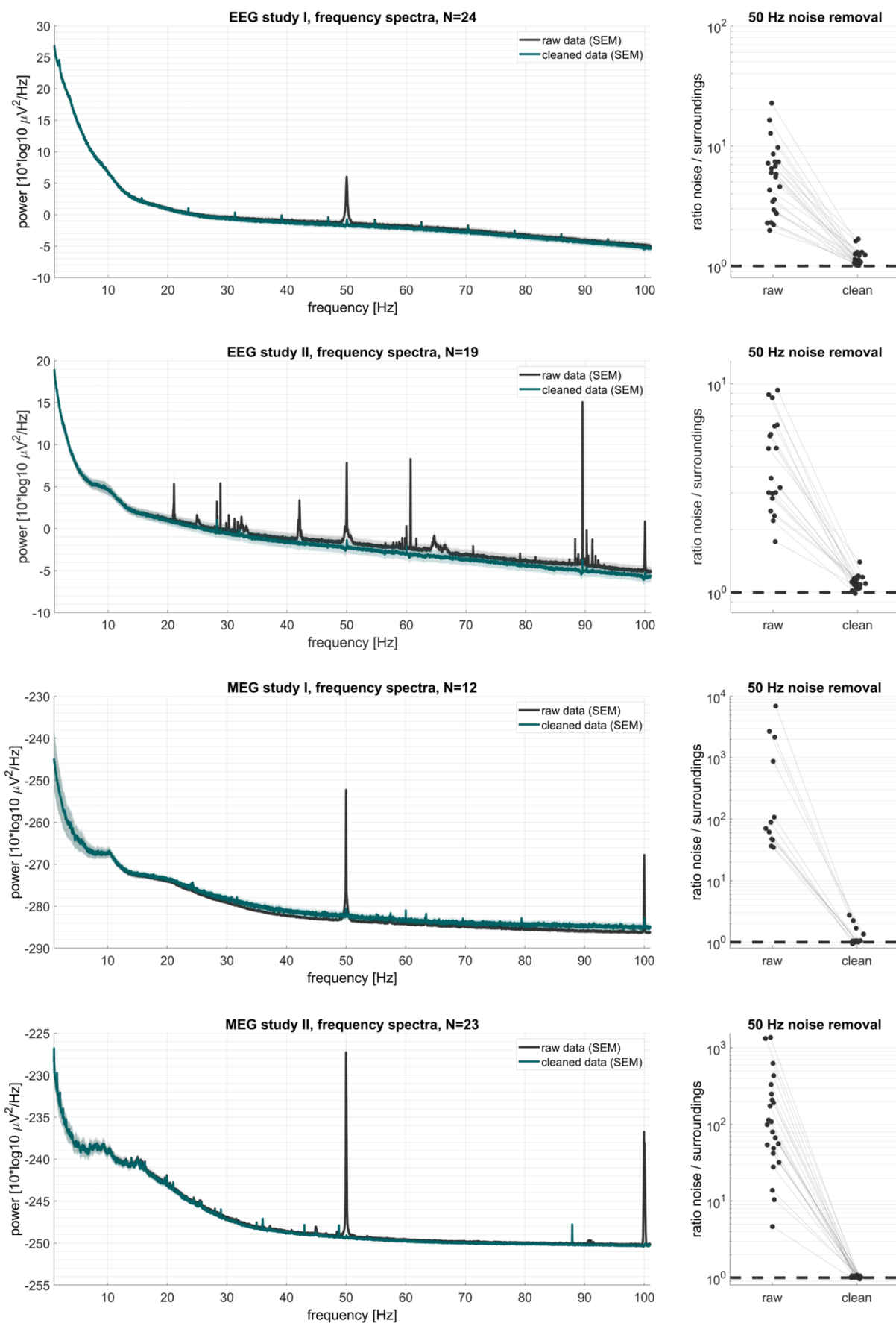
Figure 2 | Example output plots produced by Zapline-plus for 50 Hz line noise. Shown is a 9 min MEG data set from MEG study I (see section “Datasets”), with 50 Hz predefined as the noise to remove. For a detailed explanation of the individual subplots, see section “Plots”

954 **A.** Power spectrum centered around the noise frequency. **B.** Number of components removed
 955 by Zapline for each chunk. Chunks were defined as periods in which the noise was spatially
 956 stable. **C.** Specific noise frequencies detected within each chunk. **D.** Component scores,
 957 sorted in descending strength. Red line, threshold for rejection based on outlier detection. **E.**
 958 Same as A., but after removal of the noise components. **F.** Full power spectrum, depicting
 959 both the line noise and (sub-)harmonics. **G.** As E. but showing clean and noise data
 960 separately. The x-axis expresses frequency relative to the removed noise frequency, where 1
 961 indicates the noise frequency. **H.** Power spectrum of 10 Hz range below the noise frequency,
 962 indicating to what extent non-noise frequencies were affected by the cleaning.

963
 964
 965



966
 967 **Figure 3 | Example output plots produced by Zapline-plus for 21 Hz noise. Figure 3 |**
 968 **Example output plots produced by Zapline-plus for 21 Hz noise.** Shown is a 87 min EEG
 969 data set from EEG study II (see section Datasets) containing a mobile and a stationary
 970 condition. This noise artifact was present only in the first part of the data. For an explanation
 971 of the individual subplots, see section Plots. For a detailed explanation of the individual
 972 subplots, see section Plots. Conventions as in Figure 2.
 973



974

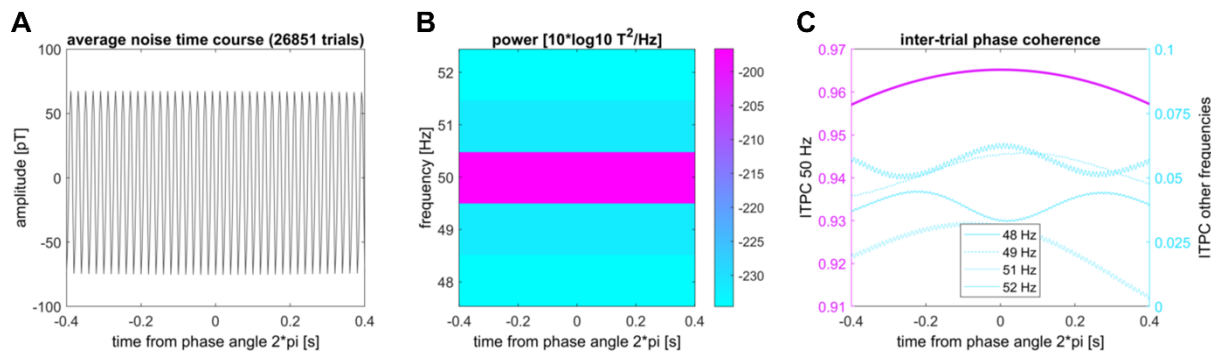
975

976

Figure 4 | Frequency spectra and 50 Hz noise removal results of the example data sets.
Rows, results for the four M/EEG data sets.datasets. Left panels: frequency spectra before

977 and after applying Zapline-plus. Right panels: ratio of power at noise / surrounding frequency
978 for raw and cleaned data. A ratio of 1 (i.e. 10^0) indicates absence of any remaining noise
979 artifact in the power spectrum.

980
981



982
983 **Figure 5 | Assessment of phase angle stability of a 50-Hz noise timeseries generated**
984 **by Zapline-plus. A.** Noise time course after averaging over short “trials” centered around the
985 2 π phase angle of 50 Hz. **B.** Spectrogram of the average trial depicted in A. **C.** Inter-trial
986 phase coherence (ITPC) of 50 Hz (y-axis on the left) and neighboring frequencies (y-axis on
987 the right).

988